

Silicon waveguided components for the long-wave infrared region*

Richard A Soref, Stephen J Emelett and Walter R Buchwald

Air Force Research Laboratory, Sensors Directorate, Hanscom Air Force Base, MA 01731, USA

Received 20 June 2006, accepted for publication 11 July 2006

Published 7 August 2006

Online at stacks.iop.org/JOptA/8/840

Abstract

We propose that the operational wavelength of waveguided Si-based photonic integrated circuits and optoelectronic integrated circuits can be extended beyond the 1.55 μm telecom range into the wide infrared from 1.55 to 100 μm . The Si rib-membrane waveguide offers low-loss transmission from 1.2 to 6 μm and from 24 to 100 μm . This waveguide, which is compatible with Si microelectronics manufacturing, is constructed from silicon-on-insulator by etching away the oxide locally beneath the rib. Alternatively, low-loss waveguiding from 1.9 to 14.7 μm is assured by employing a crystal Ge rib grown directly upon the Si substrate. The Si-based hollow-core waveguide is an excellent device that minimizes loss due to silicon's 6–24 μm multi-phonon absorption. Here the rectangular air-filled core is surrounded by SiGe/Si multi-layer anti-resonant or Bragg claddings. The hollow channel offers less than 1.7 dB cm^{-1} loss from 1.2 to 100 μm .

Keywords: silicon, germanium, waveguides, far infrared, photonic integration, optoelectronics, silica, anti-resonant, Bragg, heterostructure, hollow core

(Some figures in this article are in colour only in the electronic version)

1. Introduction

Recent investment by government (the Air Force Office of Scientific Research (AFOSR) and the Defense Advanced Research Projects Agency (DARPA)) and industry (Intel Corporation) has accelerated the development of silicon-based photonic integrated circuits (PICs) and optoelectronic integrated circuits (OEICs) for telecommunications in the 1.55 μm wavelength band. The purpose of this paper is to propose that appropriately designed Si-based PICs and OEICs can operate at a wavelength anywhere within the broad infrared spectrum stretching from 1.55 to 100 μm . This is a new 'long-wave' paradigm for silicon photonics and optoelectronics.

The opportunities for Si-based long-wave infrared (LWIR) photonics are: sensing, communications and signal-processing in the 3–5 and 8–14 μm atmospheric-transmission windows, missile detection in the 20 μm region, as well as imaging, sensing and communications in the 30–100 μm 'terahertz' regime. No doubt there are new wavelength-specific

applications in the wide 1.55–100 μm range that we have not foreseen.

2. Migration of Si-based OEICs into the 1.55 to 100 μm infrared spectral region

Noteworthy progress has already been made in bringing active Si-based devices into the LWIR, namely photodetectors, modulators and light emitters. These devices will facilitate the migration of PICs from near to far infrared. The first examples are photodetectors such as the Si/SiGe heterostructure infrared photodetectors that use Schottky-like internal photoemission to sense 3–5 μm mid infrared. There is also a family of SiGe/Si quantum well infrared photodetectors (QWIPs) that await commercialization. Laboratory demonstrations of these QWIPs have been made at wavelengths of 6 and 50 μm . At 10.6 μm , researchers in Japan successfully tested a waveguided n/n+ silicon electrooptic intensity modulator that employed electron injection through a metal-insulator-semiconductor (MIS) gate. There are also extensive experimental results on SiGe/Si quantum cascade emitters (QCEs)—cryogenically cooled devices that are expected to become quantum cascade lasers (QCLs) after more R&D

* This article was submitted to the special issue containing selected papers from the OMS'05 Conference. This special issue may be accessed online at stacks.iop.org/JOptA/8/i=7.

is performed. The principal results are from the European Community SHINE project (QCEs for 8–80 μm), and from the DARPA THz project which included two teams, one led by the University of Leeds and another led by the University of Delaware—efforts that yielded QCEs in the 50–110 μm wavelength region. Professor Kolodzey at Delaware also proved that cryo-cooled bulk silicon doped with shallow donors or acceptors will luminesce at ~ 50 μm during electrical pumping. These impurity-level Si devices have excellent laser prospects. A wide-ranging patent [1] proposes that injection-laser diodes, modulators and detectors for the 1.55–50 μm region can be constructed using GeSn/Ge multiple quantum wells grown upon SiGeSn-buffered silicon. The 1.55–8 μm lasers, detectors and modulators would use direct band-to-band transitions, while the 8–50 μm devices would be inter-subband devices.

3. Reasons for migration

We have suggested that the availability of devices discussed above provides motivation for developing LWIR silicon-based photonic integrated circuits. We believe that there are additional reasons for migrating Si-based PICs and OEICs to the wide infrared, as follows:

- (1) The waveguided chips can interface via grating couplers with incoming and outgoing ‘free space’ infrared beams, especially in the 3–5 μm and 8–14 μm atmospheric-transmission windows that are popular for military and commercial applications.
- (2) The free-carrier plasma effect is much stronger at LWIR than at 1.55 μm , which means that waveguided electrooptic modulators that function via carrier accumulation or injection will be quite efficient provided that the impurity doping of the unbiased waveguide core is kept low to minimize mode attenuation via free-carrier absorption.
- (3) Fibre optics will eventually be available across 1.6–100 μm [2, 3], enabling LWIR fibre-and-chip systems.
- (4) The PICs and OEICs enable new applications not feasible at the near infrared (NIR).
- (5) Some applications such as chemical and biological sensing are probably more effective at LWIR than at NIR.
- (6) The dimensional tolerances on LWIR devices are relaxed relative to NIR, simplifying photolithographic device fabrication.
- (7) There are scenarios for separating cryo-cooled chips from room-temperature chips; for example, the cooled OEIC would contain lasers and detectors that are coupled via LWIR fibres to an uncooled optical signal-processing network chip, or all chips could be cooled if desired.
- (8) It is likely that efficient micro-photonic, nano-photonic and plasmon-optic devices can be developed at LWIR structures that will propel a ‘Moore’s law for photonics’.
- (9) Development effort put into LWIR components will tend to improve thick-film technology and related techniques.
- (10) The compatibility of Si photonics with complementary metal oxide semiconductor (CMOS), demonstrated at 1550 nm, will undoubtedly apply to LWIR.
- (11) The integrated-component functions of filtering, splitting, combining, directional coupling, tapering, resonating, wavelength multiplexing and grating coupling, now available at 1550 nm, should work equally well at LWIR.

Looking at the categories of micro- and nano-photonics, we note that micro-photonic devices at LWIR will be on a micrometre scale, whereas nano-photonics will have either nano or micro dimensions—the semiconductor carrier-confinement structures will have nanometre dimensions, but the so-called nanostructures that offer optical confinement, such as photonic-crystal lattices, will actually have micrometre feature sizes at LWIR.

4. The LWIR waveguide challenge

If we look at the passive and active photonic components that would comprise an integrated LWIR network, these components and their interconnections would be waveguided—and if we consider the currently most popular waveguide, the silicon-on-insulator guide, we find, as described below, that the low-loss transmission range is quite limited, approximately 1.2–3.6 μm for loss $L < 2$ dB cm^{-1} , which highlights the general problem of finding guiding structures with wider IR spectral transmission. Thus, the principal challenge of LWIR chip development is to attain low-loss LWIR waveguiding on a silicon substrate. This loss problem has not been solved yet. Which LWIR waveguide geometries and materials are best is not known, nor is it clear how to minimize the attenuation due to the LWIR optical-phonon absorption that is found in group IV materials. We address these problems and focus upon the design and simulation of low-loss waveguides. Specific new heterostructures are proposed.

5. Absorption-loss spectra of materials for core and cladding

We have reviewed the materials science literature to find the experimental loss spectra of the intrinsic undoped materials from which the core and the cladding of a Si-based LWIR waveguide would be constructed. We believe that the principal core materials are Si, SiGe, SiGeSn, GeSn and Ge. Several of these can serve as claddings as well. The conventional cladding materials are glassy silicon dioxide (silica), α -silicon nitride and sapphire. However, these claddings have loss problems at LWIR as discussed below. (Air cladding does not present problems.)

Beginning with crystal silicon, figure 1, taken from Hawkins [4], illustrates the multi-phonon absorption of ‘intrinsic’ c-Si from the wavelength of 6.6 μm out to 250 μm . (The phonon assignments are shown on the graph.) From the 1.2 μm indirect bandgap of Si out to 6.6 μm the loss is quite low, and there is an excellent window in the far infrared as shown. The near/mid- and far-infrared windows are shown more clearly in figure 2 which gives the loss in dB cm^{-1} as taken from Palik’s 1–100 μm data [5]. Figure 3, taken from [4], presents the measured multi-phonon absorption of crystal germanium from the 12.5 μm wavelength out to 200 μm . The Ge loss is low from the 1.9 μm indirect edge of Ge out to 12.5 μm .

Turning to SiO₂, this amorphous material is unfortunately quite lossy throughout much of the infrared. Figure 4 presents the absorption loss of silica from the 2 μm wavelength out to 5 μm . The attenuation is high beyond 3.6 μm . The severity of SiO₂ loss over the LWIR is shown in the data of figure 5

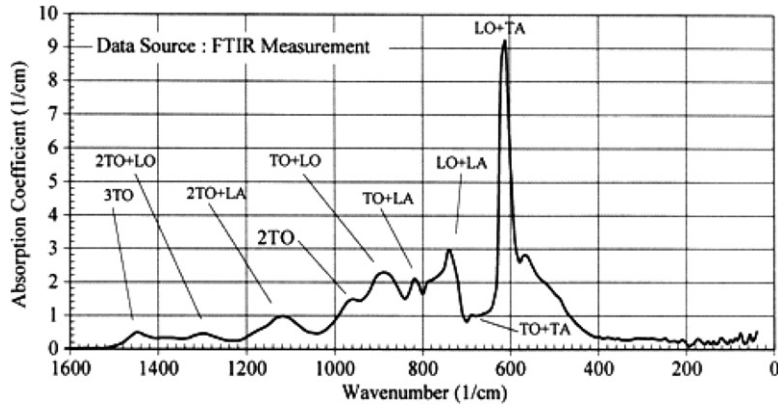


Figure 1. Absorption coefficient of undoped crystal silicon at 300 K as a function of wavenumber from 1600–40 cm^{-1} (6.6–250 μm). The experimental figure is taken from [4].

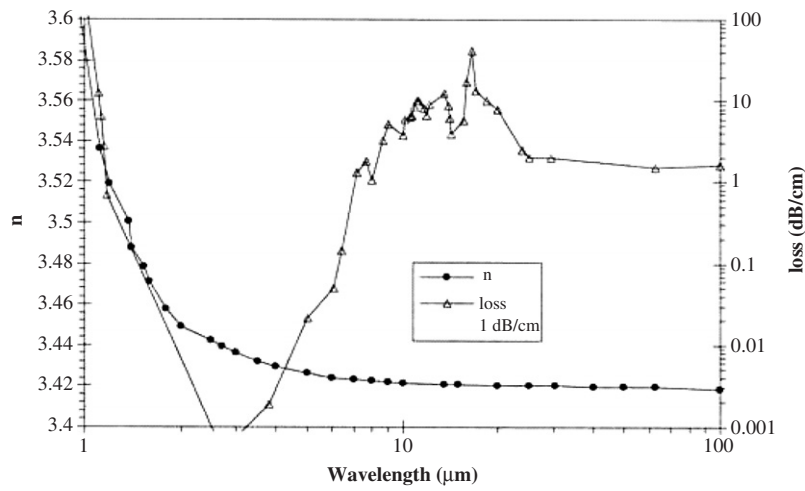


Figure 2. Refractive index and absorption loss of undoped crystal silicon at 300 K as a function of wavelength from 1–100 μm . Experimental data are taken from [5].

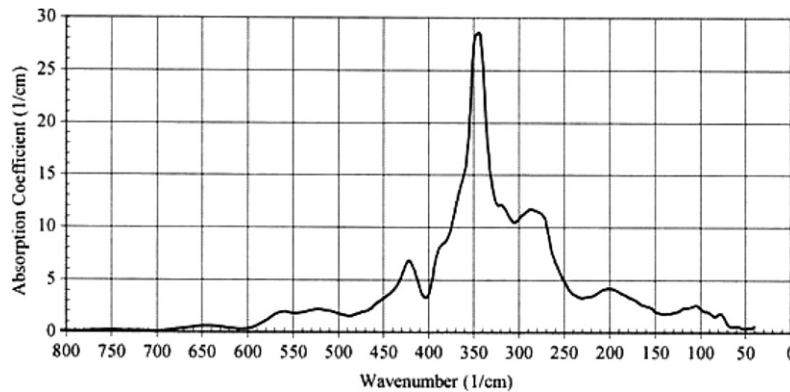


Figure 3. Absorption coefficient of undoped crystal germanium at 300 K as a function of wavenumber from 800–40 cm^{-1} (12.5–250 μm). The experimental figure is taken from [4].

taken from Palik [5]. The SiO_2 loss decreases when going from 40 to 100 μm but is still ‘too high’. As shown in figure 6, sapphire (Al_2O_3) has a better loss performance than silica over the 1–5 μm range [6]. The sapphire cutoff is taken to be $\alpha = 0.2 \text{ cm}^{-1}$ at $\lambda = 4.3 \mu\text{m}$. The nitride literature [7, 8] reveals that amorphous silicon nitride ($\text{a-Si}_3\text{N}_4$) offers low-

loss transmission from 0.22 μm out to 6.6 μm with small absorption spikes at 3.0 and 4.8 μm .

Going into more detail about the above materials, we note the following transmission ranges of ‘bulk’ material at room temperature: for crystal silicon, the loss $L < 1 \text{ dB cm}^{-1}$ over 1.2–6.9 μm and $L < 5 \text{ dB cm}^{-1}$ from 1.2–7 and 25–200 μm .

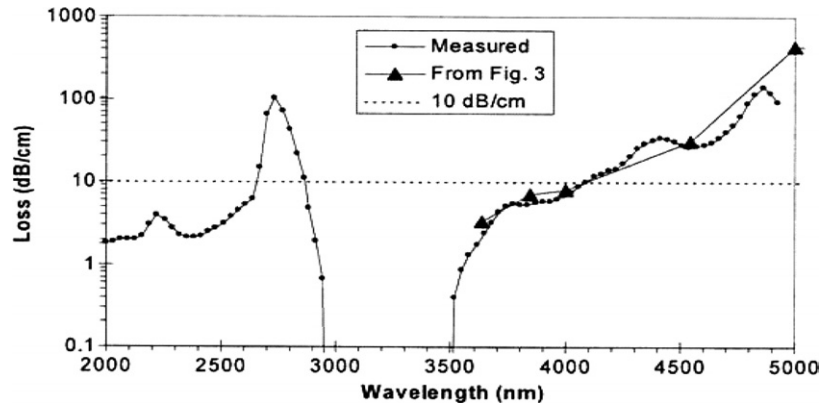


Figure 4. Absorption loss of glassy SiO_2 at 300 K as a function of wavelength from 2–5 μm .

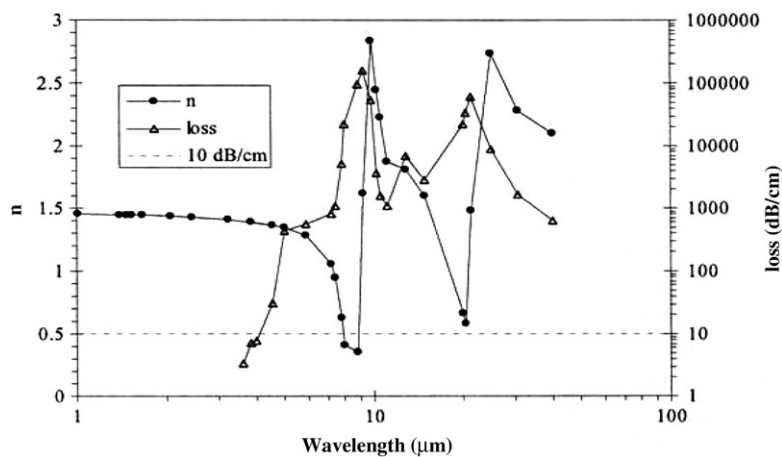


Figure 5. Refractive index and absorption loss of glassy SiO_2 at 300 K as a function of wavelength from 1–100 μm (from [5]).

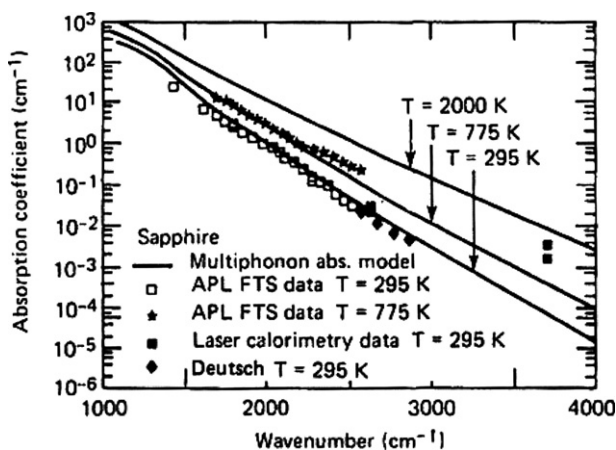


Figure 6. Absorption coefficient of crystal sapphire at 295, 775 and 2000 K as a function of wavenumber from 1000–4000 cm^{-1} (10–2.5 μm). The experimental figure is taken from [6].

For crystal germanium, $L < 1 \text{ dB cm}^{-1}$ over 1.9–16.7 μm , and $L < 5 \text{ dB cm}^{-1}$ over 1.9–16.9 μm . When Ge is cooled to 50 K, the $< 1 \text{ dB cm}^{-1}$ loss range is 1.5–18.0 μm . For glassy SiO_2 , $L < 1 \text{ dB cm}^{-1}$ over 0.25–3.6 μm , (except for the 2.6–2.9 μm spike) and $L < 5 \text{ dB cm}^{-1}$ over 0.25–3.7 μm .

For sapphire $L < 1 \text{ dB cm}^{-1}$ from 0.25–4.3 μm , and $L < 5 \text{ dB cm}^{-1}$ from 0.25–4.5 μm . For $\alpha\text{-Si}_3\text{N}_4$, $L < 1 \text{ dB cm}^{-1}$ over 0.22–6.6 μm . The favourable nitride properties lead us to propose here a new type of waveguide, silicon-on-nitride (SON) for use at the near and mid infrared. This SON guide could, for example, be made by bonding an Si wafer to a nitrided-Si wafer, followed by cutback of the top Si.

6. New and conventional silicon-based waveguides

Among the experimentally proven Si-based waveguides, we look first at those structures with a ‘silicon-like’ core. The most popular waveguide of this kind is the silicon-on-insulator (SOI) structure fashioned into the form of a strip or a rib waveguide. Other useful waveguides are SiGe upon Si, SiGeC/Si, SiGeSn/Si (and other group IV alloy heterostructures), nanocrystalline Si upon SiO_2/Si , amorphous Si upon SiO_2/Si , Si upon sapphire (SOS), SON, and high-density porous Si upon low-density porous Si which are integral on a Si wafer. There is also a silicon-upon-silicide waveguide in which a Si rib is fashioned upon a buried layer of CoSi_2 [9].

Among the newly emerging waveguides, the important ones are the photonic-crystal (PhC) silicon waveguides and the plasmon-optic waveguides consisting of a metal/dielectric or

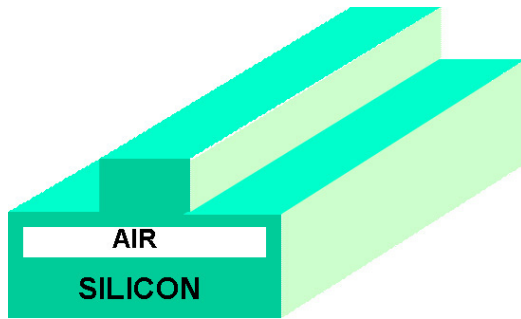


Figure 7. Proposed low-loss ‘suspended’ LWIR rib-channel waveguide consisting of a silicon membrane clad below and above by air. This waveguide is constructed from a rib-etched SOI wafer that is undercut (oxide etched away) locally beneath the rib area.

metal/dielectric/metal composite. The PhC structure can be formed in a silicon membrane suspended in air, or in a Si slab clad below by SiO_2 and clad above by air. The membrane is preferable for LWIR. PhC waveguides can be line defects in a PhC lattice or self-collimated waveguides in a defect-free dispersion-engineered PhC lattice. We suggest here that a new category, important in the LWIR context, is the hollow-core (air-filled) waveguide. Hollow waveguides differ from conventional guides because hollow guides have a cladding index that is higher than that of the core, hence the modes are ‘leaky’. Such guides confine the fundamental mode by internal or interferometric reflection of IR rays travelling at grazing incidence to the cladding. Although LWIR hollow-guide experiments have not been performed yet, we anticipate that well-designed hollow guides will transmit efficiently over a very wide IR spectrum. A fourth type of guide is the Si (or Ge) nano-slotted rib or strip. Here there is a deep vertical air-filled slot in the middle of the rib. All four types listed above are considered in this paper. Our tasks are to identify the sources of mode propagation loss within the wide IR, and to invent structures that will minimize this loss.

7. Limitations of SOI and the silicon suspended-membrane waveguide

Referring to the bulk absorption data for SiO_2 , Al_2O_3 and Si_3N_4 cited above, we can estimate the propagation loss L for SOI, SOS and SON rib waveguides by assuming that a significant fraction of the guided-mode power, such as 30% will be found in the buried insulator cladding layer. Then $L(\text{SOI}) \cong 0.7L(\text{Si}) + 0.3L(\text{silica})$ —and similarly for $L(\text{SOS})$ and $L(\text{SON})$. Since the transparency range of silica is narrower than that of the Si core, the silica imposes a limit upon the silicon. Using the above $L(\text{SOI})$ relation together with figures 1–6, we estimate that the wavelength range for which $L < 1 \text{ dB cm}^{-1}$ is 1.2–3.6 μm for SOI, (apart from a 2.6–2.9 μm spike), with ranges of 1.2–4.3 μm for SOS and 1.2–6.6 μm for SON. Although SOS and SON appear excellent for the 3–5 μm mid-infrared applications, these three ranges are too narrow for LWIR deployment, so alternative structures must be found.

The approach that comes to mind immediately is a *silicon membrane* waveguide in which the rib is suspended over an air-filled cavity comprising the lower cladding, whilst the upper

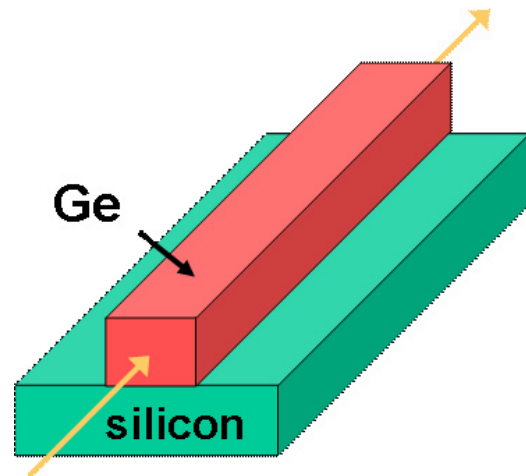


Figure 8. Proposed low-loss heterostructure LWIR strip (or rib) waveguide consisting of strain-relaxed crystal Ge grown epitaxially upon a Si substrate.

cladding is also air. This novel rib is shown in figure 7. A Si PhC membrane has already been proven effective at $\lambda = 10.6 \mu\text{m}$ by the University of Delaware group. The way in which our figure 7 guide is constructed is to etch away the buried-oxide insulating material in SOI locally under the rib, a technique that has been validated by several groups. The advantage of the membrane is that it is SOI-CMOS compatible because the SOI exists everywhere on the chip, except for the small areas beneath the various waveguides. Looking at figure 2, we estimate that the rib membrane will have losses below 1 dB cm^{-1} over 1.2–6.9 μm and 25–200 μm , which constitutes excellent LWIR performance. That is why this membrane waveguide is probably the simplest and most effective LWIR structure.

8. Proposed group IV heterostructure LWIR waveguides

We want to expand the $L < 1 \text{ dB cm}^{-1}$ wavelength range of a silicon rib-membrane waveguide, and we propose here three ways to do this. The first new device is a strip or rib waveguide of strain-relieved crystal $\text{Si}_{1-x}\text{Ge}_x$ alloy grown upon an Si substrate as illustrated in figure 8. Its loss can be estimated from a simple interpolation: $\alpha(\text{Si}_{1-x}\text{Ge}_x) = (1-x)\alpha(\text{Si}) + x\alpha(\text{Ge})$. The Ge/Si hetero-waveguide gives useful widening of the Si transparency range—the new range is 1.9–16.7 μm (assuming little mode penetration into the Si lower cladding). Thick films of Ge have already been grown upon Si in several laboratories and a commercial Ge/Si process is under way. The Ge strip/rib defects are mainly pinned at the Si/Ge interface, and a multi-micrometre layer of Ge can be grown upon an 0.2 μm Ge template. Therefore the Ge/Si LWIR waveguide appears experimentally viable, and the aforementioned 1.9–16.7 μm range seems feasible, although a bit of extra loss would arise from scattering at the Ge/Si interface and from mode-tail loss in the Si substrate, both of which would probably increase L from $\leq 1 \text{ dB cm}^{-1}$ to perhaps 2 dB cm^{-1} .

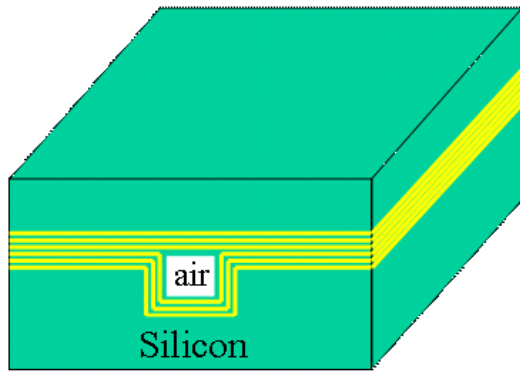


Figure 9. Proposed low-loss hollow-core (air-filled) LWIR channel waveguide consisting of an etched rectangular channel in a silicon substrate which is clad all around by alternating layers of materials A and B. A thick silicon capping layer completes the waveguide. We propose that the optimum LWIR cladding is A = SiGe and B = Si.

An alternative to Ge/Si is our proposal for a Ge membrane waveguide. This would be fabricated by starting with a germanium-on-insulator wafer (GeOI), wherein the Ge layer is separated from the Si substrate by buried SiO₂. The waveguide would be constructed by undercutting the Ge rib in the same manner that is done for the Si membrane waveguide of figure 7.

Comparing the phonon-absorption spectra in Si, Ge and Sn, we see that lattice absorption occurs at progressively longer IR wavelengths (at lower photon energies) when going from Si to Ge to Sn. That fact leads us to recommend a strip waveguide of crystal GeSn upon silicon. In this case, we expect a phonon-absorption spectrum that is red-shifted relative to that of Ge. For example, we anticipate that the alloy waveguide core composition of Ge(0.85)Sn(0.15) would have a $L \sim 1 \text{ dB cm}^{-1}$ transmission range that extends from 2.1–18 μm rather than from 1.9–16.7 μm . This remains to be verified.

9. Low-loss hollow-core LWIR waveguides

Within the past 2 years, several research groups have shown experimentally that a hollow-channel waveguide whose walls consist of multi-layer coatings will give low-loss propagation of the fundamental TE or TM grazing-incidence modes. The walls of the waveguide consist of alternating layers of material A and material B, where A has a higher refractive index than B. This air-filled hollow-channel waveguide is illustrated in figure 9. The cross section of the 3D channel can also be configured as an exposed ridge, as shown in figure 10. The hollow guides operate in two categories: those with Bragg-mirror cladding and those with ARROW (anti-resonant reflecting optical waveguide) cladding. In the Bragg case, light is total internally reflected at the multilayer. For the ARROW case, the layered wall is like a Fabry–Perot interferometric reflector. There are as few as two, or as many as $2N$ A/B layers, and the anti-resonance condition has a fairly broad spectrum.

The hollow-cladding materials reported in the literature are: either SiO₂/Si or Si₃N₄/Si [10–12]. In this paper, we propose a new type of hollow cladding—multilayers of SiGe and Si. The reason for our invention is that both SiO₂ and Si₃N₄ have rather severe absorption in the LWIR, whereas the SiGe absorption (for example, the Si_{0.5}Ge_{0.5} absorption)

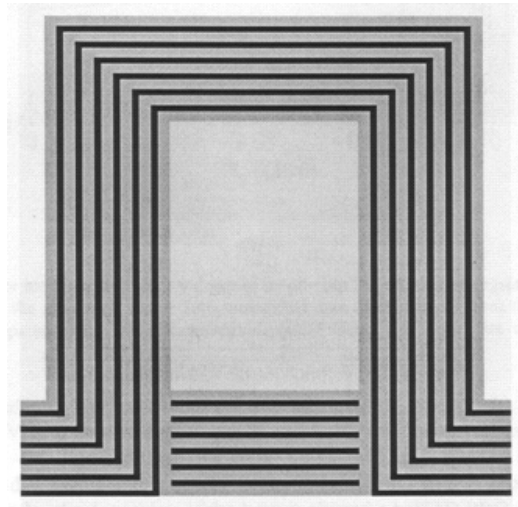


Figure 10. Cross-sectional end view of a low-loss, air-filled hollow-core LWIR channel waveguide in silicon, showing an arrangement (alternative to that in figure 9) of A/B cladding layers. This is the raised ridge approach to the rectangular core.

is significantly smaller by comparison. The SiGe/Si cladding losses are quantified below. In the far infrared, the water vapour in the air core will introduce attenuation, but the IR waveguide length will be at most a few millimetres; hence we feel that the water loss will be negligible.

The proper way to estimate the propagation loss of these waveguides is to use a 3D finite-difference time domain simulation of the waveguide transmission employing the spectral loss characteristics of both cladding materials. We have not performed this simulation, and thus can make only rough estimates of the mode attenuation. We are going to look at two sources of loss: (1) absorption in the cladding and (2) leakage due to improper waveguide geometry. Considering (1), there is penetration of the mode, roughly 10% of the power, into the lossy cladding. Therefore, 90% of the overall propagation loss is core loss (approximately zero for air) and 10% is cladding loss. The filling factor for layer A is about 50%, hence the cladding loss is about 10% of $0.5L(A) + 0.5L(B)$. For the case of *a*-Si/silica cladding, silica has peak losses of thousands of dB cm⁻¹; therefore 5% of this is still unacceptable. By the same argument, 5% of the silicon nitride loss is unacceptable.

Considering absorption in Si and SiGe, let us assume that $L(\text{Si}_{0.5}\text{Ge}_{0.5}) \cong 0.5L(\text{Si}) + 0.5L(\text{Ge})$ from figures 1 and 3. Then the maximum attenuations are: $L(\text{Si}) = 38 \text{ dB cm}^{-1}$ at the 16 μm spike, (with $L(\text{Si})$ generally less than 13 dB cm⁻¹), while $L(\text{Ge}) = 121 \text{ dB cm}^{-1}$ at the 29 μm spike, (with $L(\text{Ge})$ generally less than 52 dB cm⁻¹), from which we infer that the spike loss for $L(\text{Si}_{0.5}\text{Ge}_{0.5})$ is about 19 dB cm⁻¹ at 16 μm , plus 61 dB cm⁻¹ at 29 μm , with L less than 33 dB cm⁻¹ over the rest of the spectrum. Using the 5% multiplier for A and B discussed above, we estimate that the cladding-material loss is less than 1.65 dB cm⁻¹ over the entire 1.2–100 μm spectrum, apart from a 3 dB cm⁻¹ spike at 29 μm .

Unlike the high-contrast Si/SiO₂ system, the index contrast between Si and SiGe is ‘moderate’, for example, at $\lambda = 10 \mu\text{m}$, this index difference is 0.2914 when Si_{0.5}Ge_{0.5} is used: $n(\text{Si}, 10 \mu\text{m}) = 3.4215$, $n(\text{Si}_{0.5}\text{Ge}_{0.5}, 10 \mu\text{m}) =$

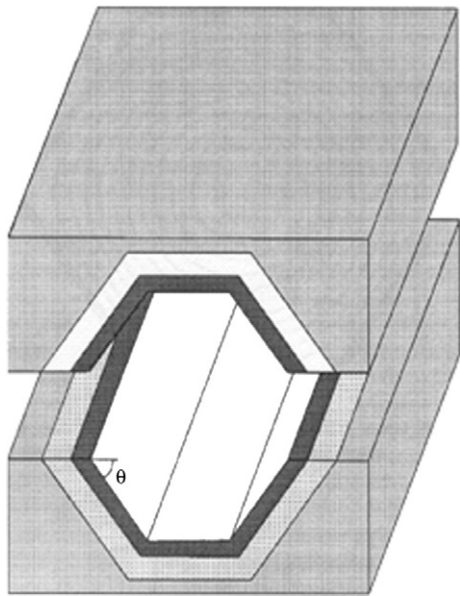


Figure 11. Perspective view of the low-loss hollow-core air-filled LWIR channel waveguide in silicon proposed by Bernini *et al*. The waveguide is assembled by fusion of top and bottom wafers of micromachined (selectively etched) silicon that each contain deposited layers A and B that form an anti-resonant interferometric reflector at the operation wavelength.

4.0043. However, the index difference is still practical for both Bragg and ARROW claddings. The paper of Bernini *et al* [7] proposes micro-machining (selective micro-etching) of Si to form the anti-resonant hollow-core 3D channel waveguide as illustrated in figure 11.

We shall now estimate the hollow-ARROW TE_o-mode leakage due to geometric factors, which occurs even when the cladding material loss is zero. We employ equation (3) of [7]. The principal ‘message’ of equation (3) is that the overall loss in cm⁻¹ is proportional to λ^4/d^5 where λ is the wavelength and d is the hollow-core diameter. Taking $\lambda = 10 \mu\text{m}$, we find that the core diameter must be greater than 12λ in order to obtain leakage loss of less than 3 dB cm^{-1} . In particular, for the Si_{0.5}Ge_{0.5}/Si anti-resonant cladding discussed above, we find that $L = 3.7 \text{ dB cm}^{-1}$ when $d = 100 \mu\text{m}$, and $L = 1.4 \text{ dB cm}^{-1}$ when $d = 140 \mu\text{m}$. It turns out that the thicknesses of the cladding layer in these cases are quite practical. Specifically, from equation (1) of Bernini [7] we estimate that the layer thicknesses of SiGe and Si are 0.64 and 0.76 μm , respectively at $\lambda = 10 \mu\text{m}$ when $d = 140 \mu\text{m}$. These would be strain-relieved crystal layers since the thickness is beyond the critical value for stable strain. Epitaxy of these layers is quite practical. Some small scattering would arise from dislocations at the SiGe/Si interface.

Looking to more futuristic devices than those in figures 9–11, we shall suggest that an alternative hollow LWIR waveguide is to construct a hollow cylindrical channel (an air-filled wire) within a 3D silicon PhC lattice, a guide analogous to a PhC fibre [13].

10. The nano-slotted rib waveguide

The Cornell group has studied the nano-slotted strip, and we propose here the nano-slotted Si rib membrane shown in

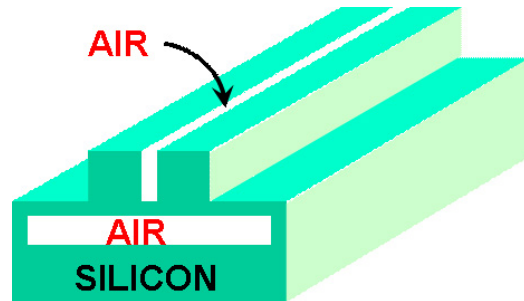


Figure 12. All-silicon suspended-membrane LWIR rib waveguide containing an air-filled slot in the Si ridge.

figure 12. For this case, where the mode is concentrated in the air-filled slot, Dr Timo Aalto has found, in an unpublished electromagnetic mode calculation, that this rib will offer a factor of two reduction in the LWIR propagation loss of a conventional rib waveguide, whatever the cause of intrinsic loss in the core [14, 15]. A detailed calculation was made at a wavelength of $10.6 \mu\text{m}$, for which the guide was two undoped crystal silicon strips, each of them 3000 nm high and 2000 nm wide, separated by a slot of width W and height 3000 nm. Air filled the slot and surrounded the Si strips. The propagation axis is Z , the width axis X and the height axis Y . For the fundamental TE mode, the field E_x is strongly concentrated in the slot, whereas the H_y field is not. The intensity distribution of $E_x \times H_y$ is an indication of mode loss, and it was found at $W = 2000 \text{ nm}$ that 74.3% of the IR power was in the two Si cores, while 25.7% was in the slot. Reducing W to 1250 nm, 32.7% was in Si and 67.3% was in the slot. Values of $W \sim 1000 \text{ nm}$ are optimum. This suggests that the waveguide in figure 12 will have 3 dB cm^{-1} mode loss at $10.6 \mu\text{m}$ if the waveguide in figure 7 has 6 dB cm^{-1} loss. In practice, smooth sidewalls are required on the slot. Nano-slotted silicon waveguides have been recommended for their large nonlinear optical effects [16].

We also propose a nano-slotted hetero-waveguide consisting of a Ge strip on an Si platform, with a nano-slot etched into the Ge strip. This would reduce the waveguide attenuation by a factor of two in the Ge-on-Si rib discussed above.

11. Alternatives to membrane waveguides

The suspended Si or Ge membrane appears quite practical for LWIR, but the infrared engineer may prefer a waveguiding structure that is ‘totally solid’ and does not have a ‘layer of air’ underneath it. This can be done with porous silicon, and with silicon-core ARROWS.

The porous silicon waveguide is integrated directly on a Si substrate. Porous silicon (PS), with its adjustable refractive index that ranges from 1.3 to 1.9 in the near infrared, can be used (1) as a lower cladding for a Si waveguiding layer or (2) as the waveguiding layer itself. Regarding (1), Arrand *et al* [17] describe the epitaxial-Si-on-PS, the Si-implanted-PS and the nitrogen-implanted-PS approaches, all of which have high loss. The case (2) is more promising and includes densified oxidized PS and controlled index PS, of which controlled index PS is the best [17]. A practical structure consists of a 65% porosity Si waveguiding layer surrounded by an upper and lower cladding layer both of 75% porosity Si [17].

Table 1. Proposed rib and strip LWIR channel waveguides based upon a silicon substrate at room temperature.

Waveguide type	Core material	Lower cladding	Upper cladding
Si/SiO ₂ /Si (SOI)	c-Si	a-SiO ₂	Air
Si/Al ₂ O ₃ /Si (SOS)	c-Si	Sapphire	Air
Si/Si ₃ N ₄ /Si (SON)	c-Si	a-Silicon nitride	Air
Si Membrane	c-Si	Air	Air
Si nano-slotted membrane	c-Si	Air	Air
SiGe/Si	Rel. c-Si _{0.5} Ge _{0.5}	Si	Air
Ge/Si	Rel. c-Ge	Si	Air
GeSn/Si	Rel. c-Ge _{0.8} Sn _{0.2}	Si	Air
Hollow core (Bragg cladding)	Air	a-Si/a-SiO ₂	a-Si/a-SiO ₂
Hollow core (Bragg cladding)	Air	Rel. SiGe/rel. Si	Rel. SiGe/rel. Si
Hollow core (Anti-resonant cl.)	Air	Rel. SiGe/rel. Si	Rel. SiGe/rel. Si
Porous-Si/Si	Low-porosity-Si	High-porosity Si	Low-porosity-Si
Si/silicide/Si	c-Si	CoSi ₂	Air
Si/epitaxial-insulator/Si	c-Si	CeO ₂ or HfO ₂	Air
Si PhC-line membrane	c-Si line defect	Air	Air
Si Phc self-collim. membr.	c-Si self-collimated	Air	Air
Si-nano-cryst./Si membr.	nc-Si	Air	Air
Si ARROW (SiGe/Si cladding)	c-Si	SiGe/Si-anti-res./Si	Air

Table 2. Estimated infrared wavelength ranges of operation at 300 K for which the fundamental-mode propagation loss is less than 2 dB cm⁻¹.

Waveguide type	Wavelength ranges of operation
Si/SiO ₂ /Si (SOI)	1.2–2.6 μm and 2.9–3.7 μm and 100–200 μm
Si/Al ₂ O ₃ /Si (SOS)	1.2–4.4 μm (and 75–200 μm at T = 77 K)
Si/Si ₃ N ₄ /Si (SON)	1.2–6.7 μm
Si membrane	1.2–8.0 μm, and 24–200 μm
Si nano-slotted membrane	1.2–9.2 μm, and 23–200 μm
SiGe/Si	1.6–12 μm and 100–200 μm
Ge/Si	1.9–16.8 μm and 140–200 μm
GeSn/Si	2.2–19 μm
Hollow core (Bragg, SiO ₂ /Si cladding)	1.2–3.9 μm
Hollow core (Bragg, SiGe/Si cladding)	1.2–200 μm
Hollow core (Anti-Res., SiGe/Si clad.)	1.2–200 μm
Porous-Si/Si	1.2–9.0 μm, and 23–200 μm
Si/silicide/Si	1.2–8.0 μm and 24–200 μm
Si/Epi insulator/Si	1.2–4.4 μm
Si PhC-line membrane	1.2–8.0 μm and 24–200 μm
Si PhC self-coll. membrane	1.2–8.0 μm and 24–200 μm
SiSi nano-crystal/Si membrane	1.2–8.0 μm and 24–200 μm
Si ARROW (SiGe/Si cladding)	1.2–8.0 μm and 24–200 μm

The silicon ARROW is another alternative. There the lower cladding for the Si rib core is a multi-layer of Si_{1-x}Ge_x and Si and Si_{1-y}Ge_y, called ARROW type-1 as specified in Soref and Ritter [18]. The practical implication is that the porous and ARROW guides will have essentially the same transparencies as the Si membrane waveguide.

The buried-silicide waveguide of Soref *et al* [9], has a silicon core clad below by a thin CoSi₂ film and clad above by air. This can be viewed as a plasmon-optic waveguide; a metal/dielectric composite. Whether the loss can be made low over the LWIR is not clear. Low loss might be feasible using a 'thin' buried-silicide layer.

12. Summary

Tables 1 and 2 summarize the proposals for LWIR waveguides and the loss estimates made in this paper. If we use the width of the low-loss spectral range(s) as a figure of merit, then we can state our findings as follows: the most practical waveguides, listed in descending order of importance, are: (1) hollow air

core with SiGe/Si cladding, (2) Si membrane, (3) Si slotted membrane, (4) Si PhC membrane, (5) Si type-1 ARROW with SiGe/Si cladding, (6) porous-Si/porous-Si, (7) Ge/Si hetero rib, (8) Si on silicide, (9) SON, (10) SOS and (11) SOI.

Acknowledgments

The authors wish to thank the Air Force Office of Scientific Research (Dr Gernot Pomrenke), for sponsorship of our in-house research at AFRL Hanscom AFB.

References

- [1] Soref R A, Kouvetakis J and Menendez J 2005 Strain-engineered direct-gap Ge/Sn_xGe_{1-x} heterodiode and multi-quantum-well photodetectors, lasers, emitters and modulators grown on Sn_ySi_zGe_{1-y-z}-buffered silicon *US Patent Specification* 6,897,471
- [2] Soref R A 2005 Silicon photonics technology: past, present and future *SPIE Photonics West, Proceedings (San Jose, CA, January 2005)* (invited plenary talk, paper 5730-02)

- [3] Soref R A 2005 Recent advances in silicon photonic components *OSA Topical Conf. Nanophotonics for Information Systems (San Diego, CA, April 2005)*
- [4] Hawkins G J 1998 Spectral characteristics of infrared optical materials and filters *PhD Thesis* Department of Cybernetics, University of Reading, UK
- [5] Palik E D 1985 *Handbook of Optical Constants of Solids* vol 1 (New York: Academic)
- [6] Thomas M E, Joseph R I and Tropf W J 1988 Infrared transmission properties of sapphire, spinel, yttria and ALON as a function of temperature and frequency *Appl. Opt.* **27** 239
- [7] Nowling G R, Babayan S E, Jankovic V and Hicks R F 2002 Remote plasma-enhanced CVD of silicon nitride at atmospheric pressure *Plasma Sources Sci. Technol.* **11** 97
- [8] Wang Y Q, Wang Y G, Cao L and Cao Z X 2003 High efficiency visible PL from amorphous Si nanoparticles embedded in silicon nitride *Appl. Phys. Lett.* **83** 3474
- [9] Soref R A, Namavar F, Kalkoran N M and Koker D M 1994 Silicon optical waveguides with buried-CoSi₂ cladding layers *Opt. Lett.* **19** 1319–21
- [10] Schmidt H, Yin D, Barber J F and Hawkins A R 2005 Hollow-core waveguides and 2-D waveguide arrays for integrated optics of gases and liquids *IEEE J. Sel. Top. Quantum Electron.* **11** 519–27
- [11] Bernini R, Campopiano S and Zeni L 2002 Silicon micromachined hollow optical waveguides for sensing applications *IEEE J. Sel. Top. Quantum Electron.* **8** 106–10
- [12] Yi Y, Bermei P, Akiyama S, Duan X and Kimerling L C 2005 On-chip silicon based waveguide with light guiding in low index core materials *Proc. SPIE* **5730**
- [13] Pearce G J, J Pottage J M, Bird D M, Roberts P, Knight J C and Russell P St J 2005 Hollow-core PCF for guidance in the mid to far infra-red *Opt. Express* **13** (18)
- [14] Aalto T 2005 private communication, VTT Information Technology, Microelectronics Division, Finland
- [15] Aalto T 2004 Microphotonic silicon waveguide components *PhD Dissertation* Helsinki University of Technology Espoo, Finland, VTT Publications 553
- [16] Baehr-Jones T, Hochberg M, Wang G, Lawson R, Liao Y, Sullivan P, Dalton L, Jen A and Scherer A 2005 Optical modulation and detection in slotted Silicon waveguides *Opt. Express* **13** (14)
- [17] Arrand H F, Benson T M, Sewell P, Loni A, Bozeat R J, Arens-Fischer R, Kruger M, Thonissen M and Luth H 1998 The application of porous silicon to optical waveguiding technology *IEEE J. Sel. Top. Quantum Electron.* **4** 975–82
- [18] Soref R A and Ritter K J 1990 Silicon antiresonant reflecting optical waveguides *Opt. Lett.* **15** 792–4